

Point defects in models of amorphous silicon and their role in structural relaxation

Cristiano L. Dias,^{1,*} Laurent J. Lewis,^{1,†} and S. Roorda^{1,‡}

¹*Département de Physique et Groupe de Recherche en Physique et Technologie des Couches Minces (GCM),
Université de Montréal, Case Postale 6128, Succursale Centre-Ville, Montréal, Québec, Canada H3C 3J7*

(Dated: November 14, 2018)

We have used tight-binding molecular-dynamics simulations to investigate the role of point defects (vacancies and interstitials) on structural relaxation in amorphous silicon. Our calculations give unambiguous evidence that point defects can be defined in the amorphous solid, showing up as anomalies in the valence-charge/Voronoi-volume relation. The changes in the radial distribution functions that take place during annealing are shown to be in close agreement with recent, highly-accurate x-ray diffraction measurements. Our calculations provide strong evidence that structural relaxation in *a*-Si proceeds by the mutual annihilation of vacancies and interstitials, i.e., local structural changes rather than an overall relaxation of the network.

Submitted to *Physical Review Letters*

PACS numbers: 61.43.Dq, 61.43.Bn, 71.55.Jv

The amorphous phase of tetrahedral covalent semiconductors is usually described in terms of an ideal continuous random network (CRN),¹ which is fully connected and perfectly fourfold coordinated; in this model, the angular and radial distributions differ only slightly from their crystalline counterparts at short range. Yet, the atomic structure of these materials — and in particular that of the prototypical amorphous silicon (*a*-Si) — has not been completely resolved and the analogy with the CRN not fully established. In particular, the presence of point defects in the network and their role during structural relaxation remains unclear. This is the problem we address here.

A striking similarity has been noted in *a*-Si between the changes induced by annealing (structural relaxation) and those associated with the removal of damage caused by radiation in *crystalline* Si.² This has led to the suggestion that point defects such as vacancies and interstitials (i) do exist in *a*-Si and (ii) are closely related to structural relaxation. Experimental evidence for the existence of such defects, and their role in relaxation, is based on the kinetics of heat release upon annealing,² Mössbauer spectroscopy,³ Cu solubility and diffusion,⁴ and, more recently, high-energy X-ray diffraction (XRD) measurements.⁵ In the latter experiment, the radial distribution function (RDF) of *pure*, ion-implanted *a*-Si was measured with very high precision, both before and after annealing. Both samples were found to be undercoordinated and *equally dense*; the average coordination number was found to increase from 3.79 to 3.88 upon annealing. This, as well as other details of the RDFs, was interpreted in terms of the mutual annihilation of vacancies and interstitials during relaxation, which brings about an increase in the average coordination number without affecting the density.

The concept of point defects provides an attractive perspective for understanding the structure of amorphous semiconductors, since it is an extension of well-known ideas developed for the corresponding crystalline phases.

However, some questions remain before this interpretation can be fully accepted. In particular, can theory provide further evidence for the existence of point defects in these materials, and can they be held responsible for structural relaxation? What are the structural and electronic properties of vacancies and interstitials in amorphous semiconductors? In this Letter, we demonstrate, based on quantum-mechanical tight-binding simulations, that the interpretation of structural relaxation in *a*-Si in terms of point defects is indeed correct. We propose specific criteria for identifying point defects and show that the changes in the RDF observed in the XRD experiments can be reproduced in detail if defects are assumed to exist and to annihilate.

Our study is based on an atomistic description of the material. We employed, as a starting point, a CRN model containing 216 atoms prepared using a modified Wooten-Winer-Weaire algorithm⁶ and the empirical Stillinger-Weber potential. This sample was then relaxed using tight-binding molecular dynamics⁸ (TBMD) at constant volume. The TBMD scheme ensures a proper, and “affordable”, description of the energetics of the material, while also providing information on the electronic structure; *ab initio* simulations are out of reach given the size of the simulations needed for the present study. The specific implementation of TBMD we used is that of Kwon *et al.*,⁹ which is cut-off at 4.18 Å, i.e., beyond the second-neighbour shell. The TBMD-relaxed sample has a density of 0.047 atoms Å⁻³, is perfectly fourfold coordinated, and the width of the angular distribution is a minuscule 10.30 °. This model will be taken as representing the fully-relaxed material.

In order to assess the role of point defects on relaxation, we also prepared “as-made” samples by introducing, by hand, a number of defects in the fully-relaxed sample. A vacancy is created, simply, by removing one atom from its equilibrium position, and an interstitial by adding an atom to the CRN. For the latter case, there exist many possibilities; we chose configurations closest

to the dumbbell, as this is the one with the lowest energy in the crystal.⁷ After the introduction of each defect, the system was fully relaxed. For vacancies, a static relaxation was found to be sufficient. For interstitials, the relaxation is sensitive to initial conditions; a simulated annealing algorithm was used to scan the energy landscape for a global minimum by quenching slowly from 300 K to 0 — the temperature was scaled down by a factor of 0.997 at every timestep = 1.08×10^{-15} s. It should be stressed that a detailed study of the complete path from the as-made to the fully-relaxed material is beyond the reach of atomistic simulations.

Altogether, 40 samples, each containing a single vacancy or a single interstitial (located at random) were prepared. In order to demonstrate that defects do exist, it is necessary to be able to locate them with reasonable confidence in the structure, *without a priori knowledge*. Evidently, no criterion will give a perfect score, as there will always be marginal cases due to the continuously disordered nature of the material. We have found that a criterion based solely on distance — e.g., to identify clusters of threefold atoms which may signify the presence of a vacancy — are not sufficiently robust for this purpose. Nevertheless, it is possible to identify defects by looking for correlations between local properties; the assumption, which we have verified, is that the presence of a defect is felt more strongly at short range. In particular, defects are expected to have a sizeable effect on the volume available to neighbouring atoms¹⁰ — the Voronoï volume — as well as on their valence charges.^{11,12}

To illustrate this point, we plot, in Figs. 1(a) and (b), the Voronoï volumes and valence charges of all atoms for the fully-relaxed sample (crosses) as well as two defective samples, each containing a single vacancy (squares); as will be shown below, these particular samples are typical of the set we generated. *Modulo* some dispersion, a clear correlation can be observed, *for most atoms*, between the volume and the valence charge. Both quantities are well bounded and the valence charge decreases with the Voronoï volume. This can be understood as follows: The Voronoï volume is proportional to the cube of the mean nearest-neighbour distance; thus, small Voronoï volumes are related to large ion-ion repulsions which can only lead to stable structures if screened by large amounts of valence electrons.

For some atoms, however, the correlation fails: some points — all of which belonging to the defective samples — clearly fall outside the main region. Examination of ball-and-stick models of the structures (insets) reveals that these atoms are spatially correlated, and in fact sit near the sites where the vacancies were created. We note that in one case, Fig. 1(b), the “peculiar” atoms do not possess a particularly large volumes (two of them are fivefold coordinated and the other is fourfold), while they do in the case of Fig. 1(a) (with all four atoms threefold coordinated); the Voronoï volume, therefore, is *not* a good probe of the presence of vacancies, in contrast to the situation in crystalline material.

Having established that vacancies can be identified in *a*-Si without *a priori* knowledge of their position, we now present a statistical analysis of all 20 samples containing a vacancy. Fig. 1(c) shows the correlation between valence charge, Voronoï volume, and coordination (as determined by a distance cutoff argument). Again, most atoms are found to belong to the main region, but a number of data points fall outside of it. Ball-and-stick models of the atomic structures reveal, again, that these points correspond to atoms surrounding vacancies. The particular examples of Fig. 1(a) and 1(b) are thus representative of all samples studied. Similar observations apply to interstitial-type defects, which we do not show here for lack of space.

The distribution of points outside the main region is found to correlate to coordination: Threefold-coordinated atoms (squares) tend to have large volumes and exhibit a “bimodal” distribution of valence charge — either large or small compared to the atoms in the main region. Fivefold atoms (circles), in contrast, occupy relatively small volumes and are surrounded by low amounts of valence charge. The volume and valence charge of fourfold-coordinated atoms, finally, present no peculiarity; their distribution must be taken as inherent to the amorphous structure. Thus, while vacancies are predominantly associated to threefold-coordinated atoms, as is the case in crystalline systems, fivefold-coordinated atoms can also signify the presence of a vacancy in the amorphous phase.

We have demonstrated that defects are stable entities that can be identified in amorphous structures. We move on to assess their role in relaxation by comparing the RDFs of models for the as-implanted and the annealed states, displayed in Fig. 2, and constructed as follows: We first define a *local*, atom-dependent RDF, $J_i(r)$, which is the number of particles per unit length at distance r from atom i . This can then be used to compute the RDF associated to a particular vacancy, which is done by summing the $J_i(r)$ of all atoms located within a distance d from the vacancy; this will be labeled $J_V^d(r)$. Likewise, we may define a $J_I^d(r)$ for interstitials. We may now combine J_V^d and J_I^d into the *total* RDF $J(r)$ of a sample containing N_V vacancies and N_I interstitials, on average $2d$ apart:

$$J(r) = n_V J_V^d(r) + n_I J_I^d(r) \quad (1)$$

where $n_V = N_V/(N_V + N_I)$ and $n_I = N_I/(N_V + N_I)$. The latter expression is formally equivalent to the usual RDF for a sample containing a density ρ of defects with relative concentrations of n_V vacancies and n_I interstitials. For proper statistics, J_V^d and J_I^d were averaged over many samples — 20 with a vacancy and 20 with an interstitial. There is a single defect per sample and defect-defect interactions are ignored. Our results are therefore valid in the limit of low defect densities, the latter being determined by the value of d as $\rho = 1/\frac{4}{3}\pi d^3$.

We now examine the structural changes brought about by the annihilation of defects. We assume here that the

structure of as-implanted and annealed samples are similar, except for the defect density and relative concentration. Thus, we can mimic both states of the material by simply varying d and n_V (or n_I). The precise form of the evolution from one state to the other can only be obtained through a detailed analysis of the atomic mechanisms that take place during annealing, which is beyond the reach of current simulations.

As noted earlier, the XRD measurements of Laaziri *et al.*⁵ suggest that the structural relaxation between as-implanted and annealed samples proceeds by the annihilation of point defects, more precisely the diffusion and recombination of vacancies and interstitials, which not only cause the coordination to increase, but also is such that the density is conserved. Thus, it must be the case that

$$N_V^{\text{ann}} = N_V^{\text{imp}} - N_I^{\text{imp}}, \quad (2)$$

where N_V^{imp} and N_I^{imp} are the number of vacancies and interstitials in the as-implanted sample, respectively, and N_V^{ann} is the number of vacancies in the annealed material; we assume here that all interstitials annihilate with vacancies, $N_I^{\text{ann}} = 0$, which imposes $n_V^{\text{imp}} \geq 0.5$.

Because density, and thus volume, is conserved during annealing, it must also be the case that

$$N_V^{\text{ann}}(d^{\text{ann}})^3 = (N_V^{\text{imp}} + N_I^{\text{imp}})(d^{\text{imp}})^3 \quad (3)$$

where $2d^{\text{imp}}$ and $2d^{\text{ann}}$ are the average distances between defects in the as-implanted and annealed sample, respectively. Combining eqs. 3 and 2, we thus have

$$d^{\text{ann}} = d^{\text{imp}} \sqrt[3]{\frac{N_V^{\text{imp}} + N_I^{\text{imp}}}{N_V^{\text{imp}} - N_I^{\text{imp}}}} \quad (4)$$

The above constraints reduce from 6 to 3 the number of parameters needed to calculate the RDF of the as-implanted and annealed materials, viz. N_V^{imp} , N_I^{imp} and d^{imp} .

We now demonstrate that the mutual annihilation of vacancies and interstitials are responsible for the changes observed during structural relaxation, i.e., increase in coordination number of the first and second neighbour peaks in the RDF and corresponding decrease of the “noise” in-between those peaks. We show in Fig. 2 the simulated RDFs for the as-implanted and annealed models, using $n_V^{\text{imp}} = \frac{2}{3}$ (and thus $n_I^{\text{imp}} = \frac{1}{3}$) and $d^{\text{imp}} = 5.5$ Å. The corresponding densities of defects are 3.1 at.% for the as-implanted material and 1.0 at.% for the annealed one, of the same order as those inferred from the experiments of Laaziri *et al.*⁵

We indeed observe, in Fig. 2, a decrease of the “noise” in between the first and second-neighbour peaks and an increase in the amplitude of the second peak following the annihilation of defects. Quantitatively, the coordination of the second peak — computed by fitting the first half to a Gaussian — increases by 0.43, in good agreement with

experiment (0.28) considering the “error bars” inherent to both approaches.

Concerning the first peak, now, an analysis of the as-implanted sample shows that the large- r tail is overestimated when compared to experiment. This is to a large extent an artifact of the computational approach, as complete relaxation of the defects — in particular the interstitials — is extremely difficult. In order to eliminate these artifacts, we follow the same procedure as that used to analyze the experimental RDF: we evaluate the coordination of the nearest-neighbour shell by fitting the first peak to a Gaussian lineshape and integrating. We find the coordination to increase by 0.06 from $Z = 3.91$ in the as-implanted sample to $Z = 3.97$ in the annealed sample. This difference is very significant: for $Z = 3.91$, one atom in 11 is, on average, threefold coordinated, while the proportion drops to one in 33 for $Z = 3.97$. Taking error bars into account, this change in coordination is in excellent agreement with the experimental value of $3.88 - 3.79 = 0.09$. It should be noted that the precise correspondance between experimental and model as-implanted samples is impossible to establish; we are really only interested in relative changes upon annealing.

The agreement between model and experiment — and thus the interpretation of relaxation in terms of point-defect annihilation — is unambiguously established in the inset of Fig. 2, where we plot the *difference* between annealed and as-implanted material for both experiment (full line) and the present model (dotted line). In order to set a common reference, the positions of the first peak of the RDFs were forced to match. The coincidence between the two data sets is striking, even though the amplitudes of the various peaks is not perfect, due to the approximate character of the computational approach. The reduction of noise between first- and second-neighbour peaks is qualitatively reproduced, and even such fine details as the small peaks or shoulders in the second-neighbour shell (3.25–4.0 Å), indicated by arrows, are correctly reproduced. These results provide strong evidence that point-defect annihilation is, indeed, the mechanism responsible for structural relaxation in amorphous silicon.

In summary, we have demonstrated, based on TBMD calculations of point defects in amorphous silicon, that there exists a correlation between the valence charge and the Voronoï volume that is broken in the presence of defects. Comparison between model as-implanted and annealed samples provides strong evidence for the interpretation of structural relaxation in *a*-Si in terms of the mutual annihilation of vacancies and interstitials, which recombine such as to increase the nearest-neighbour coordination while keeping the density constant. Thus, the concept of point defects is relevant to amorphous silicon. Annealing evidently proceeds by local structural changes rather than an overall relaxation of the network.

Acknowledgments – It is a pleasure to thank Normand Mousseau and Ralf Meyer for useful discussions. This work is supported by grants from the Natural Sciences

and Engineering Research Council (NSERC) of Canada and the “Fonds pour la formation de chercheurs et l’aide à la recherche” (FCAR) of the Province of Québec. We

are indebted to the “Réseau québécois de calcul de haute performance” (RQCHP) for generous allocations of computer resources.

* E-mail: cl’dias@yahoo.com

† To whom correspondence should be addressed; e-mail: Laurent.Lewis@UMontreal.CA

‡ E-mail: sjoerd.roorda@umontreal.ca

¹ R. Zallen, *The Physics of Amorphous Solids* (Wiley, New York, 1983).

² S. Roorda, W. C. Sinke, J. M. Poate, D. C. Jacobson, S. Dierker, B. S. Dennis, D. J. Eaglesham, F. Spaepen, and P. Fuoss, *Phys. Rev. B* **44**, 3702 (1991).

³ G. N. van den Hoven, Z.N. Liang, L. Niesen, and J. S. Custer, *Phys. Rev. Lett.* **68**, 3714 (1992).

⁴ A. Polman, D. C. Jacobson, S. Coffa, and J. M. Poate, *Appl. Phys. Lett.* **57**, 1230 (1990).

⁵ K. Laaziri, S. Kycia, S. Roorda, M. Chicoine, J.L. Robertson, J. Wang, and S.C. Moss, *Phys. Rev. Lett.* **82**, 3460

(1999).

⁶ G. T. Barkema and N. Mousseau, *Phys. Rev. B* **62**, 4985 (2000).

⁷ M. Tang, L. Colombo, J. Zhu and, T. Diaz de la Rubia, *Phys. Rev. B* **55**, 14 279 (1997).

⁸ See e.g., L. J. Lewis and N. Mousseau, *Comput. Mat. Sci.* **12**, 210 (1998).

⁹ I. Kwon, R. Biswas, C. Z. Wang, K. M. Ho, and C. M. Soukoulis, *Phys. Rev. B* **49**, 7242 (1994).

¹⁰ R. Lutz and L. J. Lewis, *Phys. Rev. B* **47**, 9896 (1993).

¹¹ E. Kim, Y. H. Lee, C. Chen and T. Pang, *Phys. Rev. B* **59**, 2713 (1999).

¹² E. Kim and Y. H. Lee, *Phys. Rev. B* **51**, 5429 (1995).

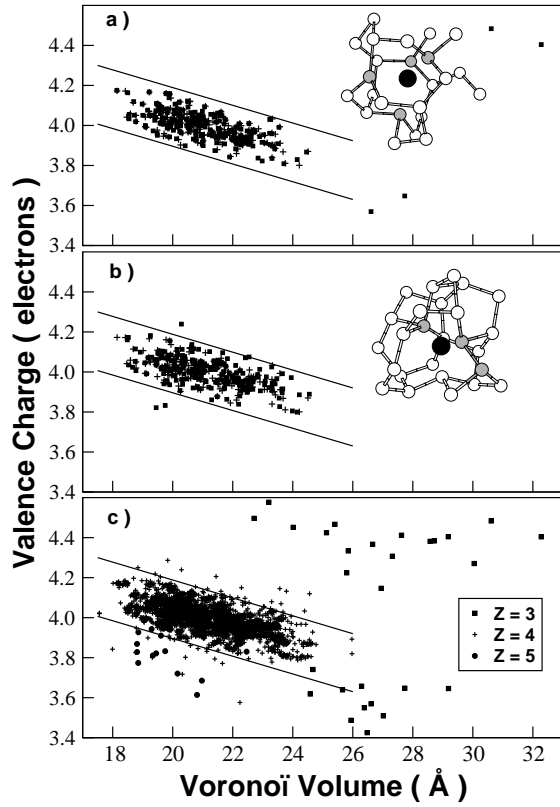


FIG. 1: Valence charge vs Voronoi volume for samples with and without vacancies. (a) and (b) are for two particular cases. Crosses are for defect-free samples while squares are for samples containing a single vacancy. The ball-and-stick models show the spatial correlation which exists between the position of the vacancy (black circle) and the positions of the atoms exhibiting an anomalous charge-volume relation (grey circles). In (c), the corresponding data is collected for all 20 samples containing a vacancy, and are sorted according to coordination, as indicated. The full lines — which are the same in all three panels — are a guide to the eye delimiting the “normal” region of correlation.

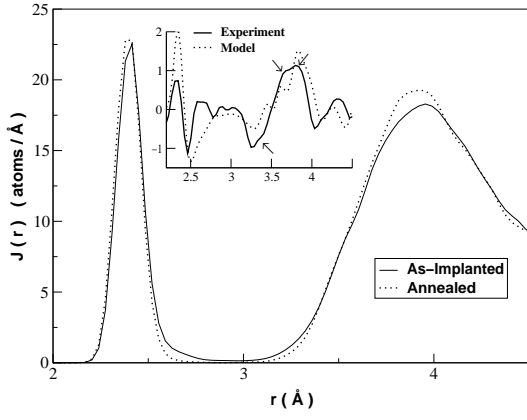


FIG. 2: RDFs of as-implanted and annealed models, for a relative concentration of vacancies of $n_v^{\text{imp}} = \frac{2}{3}$ and $d^{\text{imp}} = 5.5$ Å. The inset shows the *difference* between annealed and as-implanted RDFs for both model and experiment.